

QUANTUM SUPER-RESOLUTION BY ADAPTIVE NON-LOCAL OBSERVABLES

*Hsin-Yi Lin*¹ *Huan-Hsin Tseng*² *Samuel Yen-Chi Chen*³ *Shinjae Yoo*²

¹ Seton Hall University, Department of Mathematics & Computer Science, South Orange, NJ, USA

² Brookhaven National Laboratory, AI & ML Department, Upton, NY, USA

³ Wells Fargo, New York, NY, USA

hsinyi.lin@shu.edu, htseng@bnl.gov, yen-chi.chen@wellsfargo.com, syjoo@bnl.gov

ABSTRACT

Super-resolution (SR) seeks to reconstruct high-resolution (HR) data from low-resolution (LR) observations. Classical deep learning methods have advanced SR substantially, but require increasingly deeper networks, large datasets, and heavy computation to capture fine-grained correlations. In this work, we present the *first study* to investigate quantum circuits for SR. We propose a framework based on Variational Quantum Circuits (VQCs) with *Adaptive Non-Local Observable* (ANO) measurements. Unlike conventional VQCs with fixed Pauli readouts, ANO introduces trainable multi-qubit Hermitian observables, allowing the measurement process to adapt during training. This design leverages the high-dimensional Hilbert space of quantum systems and the representational structure provided by entanglement and superposition. Experiments demonstrate that ANO-VQCs achieve up to five-fold higher resolution with a relatively small model size, suggesting a promising new direction at the intersection of quantum machine learning and super-resolution.

Index Terms— Super-resolution, Variational Quantum Circuits, Quantum Machine Learning, Quantum Neural Networks, non-local observables, Heisenberg representations, Hermitian operators.

1. INTRODUCTION

Image super-resolution (SR) aims to reconstruct a high-resolution (HR) image from one or more low-resolution (LR) counterparts. Applications of SR span diverse fields, from natural photography [1], satellite and remote sensing [2], to medical imaging [3], where fine structural details are critical.

Classical approaches to SR include interpolation-based and sparse-representation methods [4, 5], but deep learning

This work is supported by Laboratory Directed Research and Development Program #24-061 of Brookhaven National Laboratory.

The views expressed in this article are those of the authors and do not represent the views of Wells Fargo. This article is for informational purposes only. Nothing contained in this article should be construed as investment advice. Wells Fargo makes no express or implied warranties and expressly disclaims all legal, tax, and accounting implications related to this article.

has driven dramatic improvements in recent years. Early convolutional neural network (CNN) models such as SRCNN [1], FSRCNN [6], and VDSR [7] demonstrated significant performance gains. Subsequent architectures incorporated residual connections [8, 9], dense connectivity [10], attention mechanisms [11], and transformer-based designs such as SwinIR [12]. Beyond regression models, generative frameworks have become dominant: GAN-based SR methods [8, 13] and more recently diffusion models [14] achieve perceptually realistic HR reconstructions, albeit with high computational cost and extensive data requirements.

Quantum computing offers a fundamentally different paradigm for information processing, with the potential to complement or transcend classical architectures. In particular, Variational Quantum Circuits (VQCs), which are hybrid quantum-classical models optimized through variational principles, have shown promise in quantum machine learning [15–17]. Conventional VQCs, however, rely on fixed local observables (often Pauli operators) for measurement, which limits expressivity and restricts access to the exponentially rich Hilbert space.

Recently, an *Adaptive Non-Local Observable* (ANO) framework was introduced [18], inspired by the Heisenberg picture, where the measurement operators themselves are treated as trainable Hermitian observables acting on multiple qubits. By learning both circuit parameters and observables, ANO-VQCs expand the representational capacity of quantum neural networks, enabling richer qubit interactions, enhanced feature mixing, and parameter efficiency. Importantly, non-local observables allow the readout to span different equivalence classes of Hermitian operators, thus capturing a broader range of eigenvalue spectra and providing more informative measurements than fixed Pauli observables.

In this work, we propose applying ANO-VQCs to image super-resolution. Our central insight is that non-local observables naturally serve as higher-resolution “lenses” for quantum systems: by enabling measurements across entangled multi-qubit subspaces, ANO-VQCs can extract fine-grained information that corresponds to HR details. This approach leverages the intrinsic high dimensionality of quan-

tum Hilbert space to realize perceptual improvements in SR without requiring prohibitively deep circuits or large qubit counts. By bridging recent advances in SR research [19] with adaptive quantum measurement strategies [18], this work positions ANO-based quantum circuits as a novel and resource-efficient paradigm for super-resolution.

2. ADAPTIVE NON-LOCAL OBSERVABLE VQC (ANO-VQC)

2.1. General VQC Structures

The VQC is an approach to realize QML by seeking proper unitary transformations in qubit systems to fit and learn data.

Let $\mathcal{D} = \{(x^{(j)}, y^{(j)}) \mid x^{(j)} \in \mathbb{R}^n, y^{(j)} \in \mathbb{R}\}$ be a set of classical data with $x^{(j)}$ as an input of sample j and $y^{(j)}$ as the corresponding ground truth.

The VQC fits \mathcal{D} by three steps: *encoding*, *variation*, and *measurement* (Fig. 1). Denote the set of unitary transformations in Hilbert space \mathcal{H}^n by $\mathcal{U}(\mathcal{H}^n)$. The encoding step maps a classical input $x \in \mathbb{R}^n$ into a unitary $V(x) \in \mathcal{U}(\mathcal{H}^n)$. When acting on a random initial state $|\psi_0\rangle \in \mathcal{H}^n$, $|\psi_x\rangle := V(x)|\psi_0\rangle$ is called the **encoded state** to carry the information of x . The variation step applies a parameterized unitary $U(\theta)$ to the encoded state $|\psi_x\rangle$, yielding $|\psi_{\theta,x}\rangle := U(\theta)|\psi_x\rangle$. The tunable parameters θ play a role analogous to weights in classical neural networks. By varying θ , the resulting state $|\psi_{\theta,x}\rangle$ traverses different regions of the Hilbert space \mathcal{H}^n in search of a representation that best captures the structure of the learning task.

Final measurement chooses a Hermitian matrix $H^\dagger = H$ to compute the following bilinear form as the model prediction,

$$f_\theta(x) := \langle \psi_{\theta,x} | H | \psi_{\theta,x} \rangle = \langle \psi_0 | V^\dagger(x) \underbrace{U^\dagger(\theta) H U(\theta)}_{(1)} V(x) | \psi_0 \rangle$$

to be compared with the target value y via a loss function,

$$L(\theta; \mathcal{D}) = \frac{1}{|\mathcal{D}|} \sum_{j=1}^{|\mathcal{D}|} \|f_\theta(x^{(j)}) - y^{(j)}\|^2 \quad (2)$$

In Quantum Mechanics, a Hermitian matrix H for measurement is also called an **observable**. In the VQC, an observable is chosen to be *fixed*, typically from Pauli matrices $\mathcal{P} = \{I, \sigma_1, \sigma_2, \sigma_3\}$.

On the other hand, the parametrized $U(\theta)$ is the *only* learnable component to fit \mathcal{D} by minimizing loss (2), while the encoding map V and the measurement Hermitian H remain fixed. General quantum circuit compositions employ Hadamard gate H , CNOT gate C , and rotation gates $\{e^{-\frac{i}{2}\phi\sigma_1}, e^{-\frac{i}{2}\phi\sigma_2}, e^{-\frac{i}{2}\phi\sigma_3}\}$ generated by Pauli \mathcal{P} with angle ϕ . For example, a choice of an encoding matrix can be,

$$V(x) = \bigotimes_{q=1}^n \left(e^{-\frac{i}{2}x_q \sigma_{k_q}} \circ H \right) \quad (3)$$

and a variational circuit

$$U(\theta) = \prod_{\ell=1}^L \left(\bigotimes_{q=1}^n e^{-\frac{i}{2}\theta_q^{(\ell)}\sigma_q} \right) \circ \mathcal{C}_\ell \in \mathcal{U}(\mathcal{H}^n) \quad (4)$$

with tunable parameters $\theta = (\theta_1^{(1)}, \dots, \theta_n^{(L)}) \in \mathbb{R}^{n \times L}$ (Fig. 1).

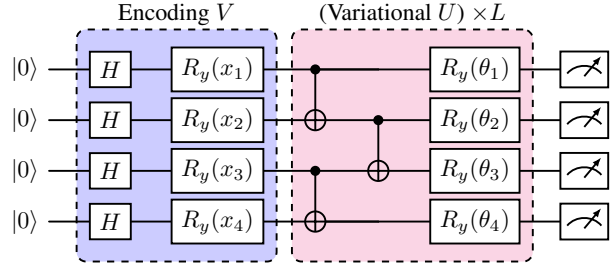


Fig. 1: A VQC diagram of (3), (4), which is also implemented in Sec. 3. The variational block represented by a pink box is repeated L times to increase the circuit depth.

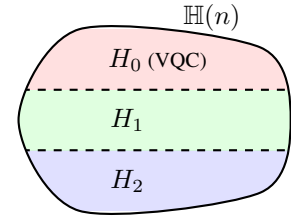


Fig. 2: Let $\mathbb{H}(n)$ denote the space of all observables represented by ANO. The conventional VQC with fixed Pauli measurements becomes a special case (an equivalent subclass) within the ANO function classes; see [18] for details.

It is demonstrated in [20] that relaxing the constraint of fixed Pauli measurements with learnable observables leads to a marked enhancement in model performance.

It is further analyzed in [18] that through the adaptation of non-local observables, the VQC formalism becomes a special case of the ANO function class (Fig. 2). Thus, k -local ANO of the following form unifies and generalizes the standard VQC,

$$H(\phi) = \begin{pmatrix} c_{11} & a_{12} + ib_{12} & a_{13} + ib_{13} & \cdots & a_{1K} + ib_{1K} \\ * & c_{22} & a_{23} + ib_{23} & \cdots & a_{2K} + ib_{2K} \\ * & * & c_{33} & \cdots & a_{3K} + ib_{3K} \\ \vdots & \vdots & \vdots & \ddots & \vdots \\ * & * & * & \cdots & c_{KK} \end{pmatrix} \quad (5)$$

where $\phi = (a_{ij}, b_{ij}, c_{ii})_{i,j=1}^K$ are arbitrary K^2 real parameters to be varied with $K = 2^k$, and the lower triangle entries are determined by the complex conjugates of the upper triangle such that $H(\phi) = (h_{ij}) = (\overline{h_{ji}}) = H^\dagger(\phi)$. (5) is a form of **k -local** observable in an n -qubit system ($k \leq n$).

The structural flexibility inherited from ANO permits the execution of complex tasks, such as resolution enhancement in image processing.

2.2. ANO-VQC for SR

Building upon the general VQC framework in Sec. 2.1, we apply ANO-VQC architecture for the quantum realization of SR. The dimensionality of LR inputs is enlarged by harnessing the expressive power of variational transformations together with learnable non-local observables. This allows the network to reconstruct HR outputs from quantum measurements.

2.2.1. Workflow Structure

The workflow of the ANO-VQC for SR is composed of the following stages:

1. **Encoding of LR images:** Each LR input image is first vectorized and embedded into the n -qubit Hilbert space by an encoding unitary $V(x)$ as in (3).
2. **Variational transformation:** The encoded state is processed by variational unitaries $U(\theta)$ defined in (4). The tunable parameters θ act to explore the quantum state space, preparing representations that are more suitable for the next measurement step.
3. **HR images by ANO:** We employ adaptive k -local observables $H(\phi)$ as in (5). Multi-qubit measurements are repeatedly performed, generating the predicted HR pixel values.

2.2.2. Learning Mechanism

The trainable parameters are:

- *variational rotation angles* $\theta = \{\theta^i\}$,
- *adaptive Hermitian observable* $\phi = \{\phi^i\}$.

The joint optimization of the variational parameters θ and the adaptive observable parameters ϕ is achieved through minimizing a reconstruction loss that measures the difference between the predicted outputs and the ground-truth HR images. To balance pixel-level fidelity with perceptual quality, we adopt a *combined loss function*:

$$\mathcal{L}(\theta, \phi) = c_1 \text{MSE} + c_2 \text{LPIPS}, \quad (6)$$

where $c_1, c_2 > 0$ are weighting coefficients. The mean squared error (MSE) term penalizes deviations in pixel intensities, ensuring accurate reconstruction of fine details. The Learned Perceptual Image Patch Similarity (LPIPS) term [21] evaluates *perceptual similarity* by comparing deep feature representations extracted from pretrained neural networks,

Table 1: Super-resolution test performance metrics for 2-local and 3-local methods Performance across different scaling factors showing degradation as scale increases.

	Scale	MSE ↓	LPIPS ↓	PSNR ↑	SSIM ↑
2-local	x3	0.42	0.16	24.13	0.84
	x4	0.62	0.19	22.32	0.76
	x5	0.80	0.22	21.18	0.66
3-local	x3	0.35	0.17	24.85	0.87
	x4	0.53	0.20	23.04	0.80
	x5	0.69	0.23	21.83	0.70

thus aligning the reconstructed outputs with human visual perception.

This combination allows the model to capture both **low-level accuracy** (via MSE) and **high-level perceptual quality** (via LPIPS), providing a more comprehensive objective for training ANO-VQC-based SR.

3. EXPERIMENTS

3.1. Experimental setup

Experiments were conducted on the **MNIST** dataset, consisting of 28×28 grayscale images of handwritten digits (0–9). Images were downsampled to 4×4 as LR inputs and upsampled to 12×12 , 16×16 , and 20×20 for $\times 3$, $\times 4$, and $\times 5$ HR targets, respectively. The proposed ANO-VQC models were evaluated on these SR tasks, with both 2-local and 3-local adaptive observables implemented to assess the impact of non-local measurement depth on reconstruction fidelity and perceptual quality.

3.2. Results

Tables 1 summarize the quantitative metrics, including MSE, peak signal-to-noise ratio (PSNR), structural similarity (SSIM), and LPIPS. Across all scaling factors, the 3-local ANO-VQC consistently achieved lower MSE and higher PSNR and SSIM than the 2-local counterpart, indicating more accurate pixel-level reconstruction. However, its LPIPS values are slightly higher, suggesting a modest perceptual degradation compared to the 2-local case. This trade-off implies that deeper non-local observables enhance reconstruction fidelity but may slightly overfit high-frequency components, resulting in perceptually sharper yet less natural details.

The improvement is most evident for the $\times 3$ SR task, where the 3-local model reached an MSE of **0.35** and an SSIM of **0.87**, compared to 0.42 and 0.84 for the 2-local variant. As the scaling factor increases to $\times 5$, both models show gradual degradation in reconstruction quality, a natural effect of larger

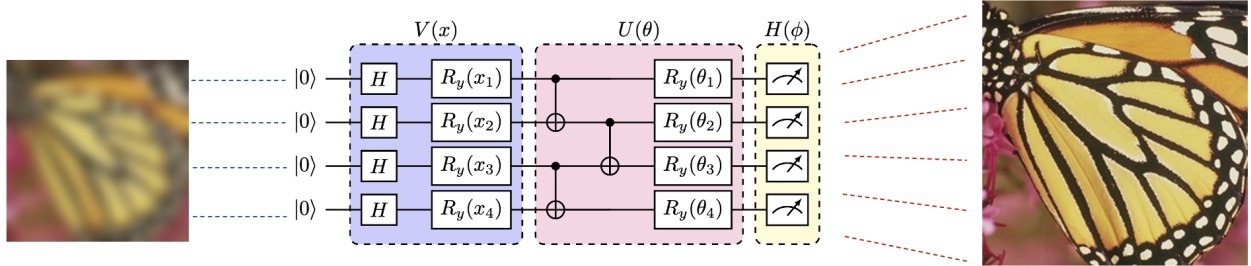


Fig. 3: ANO-VQC for SR. An LR input x is encoded by $V(x)$ into state $V(x) |\psi_0\rangle$, transformed by variational layers $U(\theta)$, and finally measured by an adaptive k -local observable $H(\phi)$ to reconstruct the HR output.

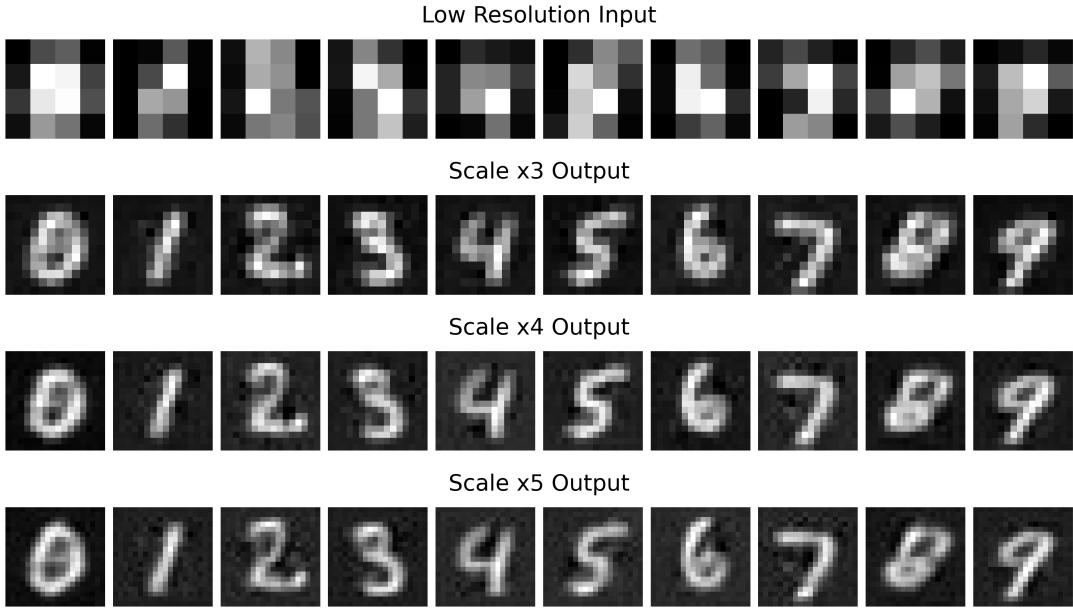


Fig. 4: Super-resolution with 3-local ANO-VQC: 4×4 LR digit inputs (top) are reconstructed into 12×12 , 16×16 , and 20×20 HR outputs in the second, third, and fourth rows.

upsampling ratios. Fig. 4 visualizes the SR outputs from the 3-local ANO-VQC.

Overall, the results highlight the advantage of using non-local measurement operators $H(\phi)$. By allowing multi-qubit Hermitian observables to adapt during training, the model explores a richer subspace of the Hilbert space, effectively enlarging the representational dimensionality.

The experimental results confirm that the proposed method effectively expands the expressive power of variational quantum circuits without requiring deeper layers or additional qubits. By optimizing both variational angles θ and Hermitian parameters ϕ , the ANO-VQC jointly learns how to transform and how to observe the quantum state for faithful image reconstruction.

4. CONCLUSION

This work introduced a quantum framework for image super-resolution based on ANO-VQCs. By jointly optimizing

variational parameters and trainable Hermitian observables, the proposed model extends the representational power of conventional VQCs, enabling adaptive multi-qubit measurements that capture fine-grained spatial correlations. Experiments on the MNIST dataset demonstrated that ANO-VQCs achieve effective reconstruction of high-resolution images from highly compressed inputs, with quantitative improvements in MSE, PSNR, and SSIM compared to fixed-observable counterparts. While 3-local observables enhance structural fidelity, a slight increase in LPIPS indicates a perceptual trade-off, highlighting the tunable balance between sharpness and visual realism.

These findings suggest that adaptive measurement design can serve as a powerful mechanism for resource-efficient quantum learning models. Future work will explore scaling ANO-VQCs to larger quantum systems, integrating hybrid classical-quantum postprocessing, and extending this approach to more complex datasets and generative vision tasks.

5. REFERENCES

- [1] Chao Dong, Chen Change Loy, Kaiming He, and Xiaoou Tang, “Image super-resolution using deep convolutional networks,” in *IEEE Transactions on Pattern Analysis and Machine Intelligence*, 2015, vol. 38, pp. 295–307.
- [2] Xiao Liu, Qiang Yuan, Kai Jiang, Jingwen He, Xin Jin, and Liang Zhang, “Ediffrs: An efficient diffusion probabilistic model for remote sensing image super-resolution,” *IEEE Transactions on Geoscience and Remote Sensing*, 2023.
- [3] Hyungjin Chung, Eun Sun Lee, and Jong Chul Ye, “Mr image denoising and super-resolution using regularized reverse diffusion,” *IEEE Transactions on Medical Imaging*, vol. 42, no. 4, pp. 1207–1218, 2022.
- [4] Jianchao Yang, John Wright, Thomas Huang, and Yi Ma, “Image super-resolution via sparse representation,” *IEEE Transactions on Image Processing*, vol. 19, no. 11, pp. 2861–2873, 2010.
- [5] Chih-Yuan Yang, Chao Ma, and Ming-Hsuan Yang, “Single-image super-resolution: A benchmark,” in *ECCV*, 2014, pp. 372–386.
- [6] Chao Dong, Chen Change Loy, and Xiaoou Tang, “Accelerating the super-resolution convolutional neural network,” in *ECCV*. Springer, 2016, pp. 391–407.
- [7] Jiwon Kim, Jung Kwon Lee, and Kyoung Mu Lee, “Accurate image super-resolution using very deep convolutional networks,” in *CVPR*, 2016, pp. 1646–1654.
- [8] Christian Ledig, Lucas Theis, Ferenc Huszár, Jose Caballero, Andrew Cunningham, Alejandro Acosta, Andrew Aitken, Alykhan Tejani, Johannes Totz, Zehan Wang, and Wenzhe Shi, “Photo-realistic single image super-resolution using a generative adversarial network,” in *CVPR*, 2017, pp. 4681–4690.
- [9] Yulun Zhang, Kunpeng Li, Kai Li, Lichen Wang, Bineng Zhong, and Yun Fu, “Image super-resolution using very deep residual channel attention networks,” in *ECCV*, 2018, pp. 286–301.
- [10] Tong Tong, Gen Li, Xiejie Liu, and Qinquan Gao, “Image super-resolution using dense skip connections,” in *ICCV*, 2017, pp. 4799–4807.
- [11] Bin Niu, Wengang Wen, Wenqi Ren, Xiangyu Zhang, Liang Yang, Shiqi Wang, Kai Zhang, Xiaochun Cao, and Heng Shen, “Single image super-resolution via a holistic attention network,” in *ECCV*, 2020, pp. 191–207.
- [12] Jingyun Liang, Jiezhang Cao, Guolei Sun, Kai Zhang, Luc Van Gool, and Radu Timofte, “Swinir: Image restoration using swin transformer,” in *ICCV*, 2021, pp. 1833–1844.
- [13] Xintao Wang, Ke Yu, Shixiang Wu, Jinjin Gu, Yihao Liu, Chao Dong, Yu Qiao, and Chen Change Loy, “Esrrgan: Enhanced super-resolution generative adversarial networks,” in *ECCV Workshops*, 2018.
- [14] Chitwan Saharia, Jonathan Ho, William Chan, Tim Salimans, David J. Fleet, and Mohammad Norouzi, “Image super-resolution via iterative refinement,” *IEEE Transactions on Pattern Analysis and Machine Intelligence*, vol. 45, no. 4, pp. 4713–4726, 2022.
- [15] M. Cerezo, A. Arrasmith, R. Babbush, S.C. Benjamin, S. Endo, K. Fujii, J.R. McClean, K. Mitarai, X. Yuan, L. Cincio, and P.J. Coles, “Variational quantum algorithms,” *Nature Reviews Physics*, vol. 3, no. 9, pp. 625–644, 2021.
- [16] Jarrod R McClean, Jonathan Romero, Ryan Babbush, and Alán Aspuru-Guzik, “The theory of variational hybrid quantum-classical algorithms,” *New Journal of Physics*, vol. 18, no. 2, pp. 023023, 2016.
- [17] Kishor Bharti, Alba Cervera-Lierta, The Htet Kyaw, Tobias Haug, Shah Alperin-Lea, Abhinav Anand, Matthias Degroote, Henri Heimonen, Jakob S. Kottmann, Tim Menke, et al., “Noisy intermediate-scale quantum algorithms,” *Reviews of Modern Physics*, vol. 94, no. 1, pp. 015004, 2022.
- [18] Hsin-Yi Lin, Huan-Hsin Tseng, Samuel Yen-Chi Chen, and Shinjae Yoo, “Adaptive non-local observable on quantum neural networks,” *arXiv preprint arXiv:2501.05663*, 2025.
- [19] Z. Wang, J. Chen, and S.C.H. Hoi, “Deep learning for image super-resolution: A survey,” *IEEE Transactions on Pattern Analysis and Machine Intelligence*, vol. 43, no. 10, pp. 3365–3387, 2021.
- [20] Samuel Yen-Chi Chen, Huan-Hsin Tseng, Hsin-Yi Lin, and Shinjae Yoo, “Learning to measure quantum neural networks,” in *2025 IEEE International Conference on Acoustics, Speech, and Signal Processing Workshops (ICASSPW)*. IEEE, 2025, pp. 1–5.
- [21] Richard Zhang, Phillip Isola, Alexei A. Efros, Eli Shechtman, and Oliver Wang, “The unreasonable effectiveness of deep features as a perceptual metric,” in *Proceedings of the IEEE Conference on Computer Vision and Pattern Recognition (CVPR)*, 2018, pp. 586–595.